

CFD-Based Gust Response Analysis of Free Elastic Aircraft

DANIELLA E. RAVEH¹

(Received: July 16, 2009. Revised: Apr. 21, 2010. Accepted: Apr. 28, 2010)

Abstract

The study presents two novel approaches for gust response analysis of elastic free aircraft configuration using computational fluid dynamics (CFD) tools. The *direct approach* involves full aeroelastic dynamic simulation within a CFD run. The *hybrid approach* involves computing rigid sharp-edge gust responses in a CFD run, evaluating the gust input forces due to arbitrary gust profiles via convolution using those rigid sharp-edge gust responses, and applying a linear aeroelastic feedback loop. The latter is highly computationally efficient, as only one relatively short CFD run is required for the computation of the sharp-edge gust responses, after which responses to arbitrary gust profiles can be computed in seconds. The former is more elaborate and time consuming, and can be used in cases in which the elastic response may be non-linear. The two methods are demonstrated by computing responses to one-minus-cosine gust inputs of a transport aircraft model.

1. Introduction

Gust response analysis plays a major role in aircraft structural design, as gust loads typically control the wing-design of large aircraft. Production methods for dynamic gust analysis usually rely on linear, frequency-domain, panel-method aerodynamic methods that are used in conjunction with the frequency-domain formulation of the aeroelastic equations of motion. For time-response simulations, or for aeroservoelastic analyses, time-domain state-space models can be extracted by rational function approximation[5, 4], or other reduced-order modeling techniques.[2, 15] However, this extraction is not straightforward.[5, 2]

The existing gust analysis methods are especially challenged when new technologies and configurations are designed, such as the High Altitude Long Endurance (HALE) aircraft configuration. A HALE wing is typically of very high aspect ratio, extremely elastic, and therefore highly susceptible to large deformations and dynamic elastic responses when subjected to atmospheric turbulence.

A well-known case of structural failure of a HALE configuration due to unfavorable response to atmospheric turbulence is that of the Helios remotely piloted vehicle. This proof-of-concept airplane crashed in June 2003, after take-off from Kauai, Hawaii, encountering turbulence, and morphing into an unexpected high dihedral configuration that made the aircraft unstable in a divergent pitch mode.

The Helios mishap investigation report[8] states that the root causes of the mishap include the lack of adequate analysis methods to predict the configurations high sensitivity to disturbances that may lead to configurational changes and instability. Quoting the investigation report: The aircraft represents a non-linear stability and control problem involving complex interactions among the flexible structure, unsteady aerodynamics, flight control system, propulsion system, the environmental conditions, and vehicle flight dynamics. The analysis tools and solution techniques were constrained by conventional and segmented linear methodologies that did not provide the proper level of complexity to understand the technology interactions on the vehicles stability and control characteristics. As a result, key recommendations include: "Develop more advanced,

¹ Faculty of Aerospace Engineering, Technion - IIT
Haifa 32000, Israel

multidisciplinary (structures, aeroelastic, aerodynamics, atmospheric, materials, propulsion, controls, etc.) *time-domain* analysis methods appropriate to highly flexible, morphing vehicles . . .”

The current study proposes a method of using CFD tools for dynamic gust response analysis, both via direct numerical simulation, and via reduced-order modeling (ROM) of the aerodynamic rigid gust forces. The advantages of using CFD tools for gust response analysis are four fold: a) CFD analysis offers various levels of accurate aerodynamic modeling, adequate for various flight regimes; b) CFD models are unsteady time-domain models and therefore are suitable for dynamic response analysis; c) CFD methods accurately predict the development of gust forces, as they account for the propagation of the gust interference throughout the flow field in the speed of sound; and d) Navier-Stokes, turbulent CFD models are capable of predicting the aerodynamic load decrease associated with flight at high angles of attack, close to stall. Therefore, when used for gust analysis, such methods can better predict the gust loads at low-speed flights, and allow for high-fidelity aeroelastic design.

In recent years, several studies have addressed CFD-based gust response analysis. Zaide and Raveh[17] simulated time histories of the aerodynamic response of two-dimensional airfoils to arbitrary gust inputs, and validated the gust responses by comparison to the closed-form Kussner functions in the subsonic and transonic flow regimes. Gust velocity inputs were introduced into the EZNSS[7] (Elastic Zonal Navier-Stokes Simulation) CFD code using the *Field Velocity* method, proposed by Parameswaran and Baeder[9] and practiced by Singh and Baeder.[13, 14] Yang and Obayashi[16] presented CFD gust simulation of a complete aircraft configuration to one-minus-cosine gust profile, using two rigid-body degrees of freedom of pitch and plunge, with and without elastic effects.

Raveh[12] presented CFD simulation and reduced-order modeling of a clamped rigid wing in response to traveling gust excitations. Four ROMs were evaluated: a convolution model that is based on CFD computed sharp-edge gust response, two parametric ARMA (Auto Regressive Moving Average) and state-space models, and a frequency response model. Models of the lift coefficient, root bending moment, and gust generalized aerodynamic forces were developed and used to compute responses to discrete and continuous gust excitations. The purpose of that study was to examine the suitability (that is, the accuracy, the computational cost, and the ease of application) of various ROMs, for replacing a full CFD simulation. Validation was achieved through comparison of the responses from these models to those computed directly in CFD simulations. Convolution models were found to be very attractive for gust response applications, thus they are applied and examined in the current study for gust analysis of a free elastic aircraft configuration.

The current study proposes and examines two CFD-based gust analysis methods: a) a complete CFD aeroelastic simulation, including elastic and rigid body motions, and b) a hybrid aeroelastic simulation in which the rigid gust forces are CFD-based (provided by convolution of the gust velocity profile with CFD-based sharp-edge gust responses), and the aeroelastic feedback is based on linear aerodynamics (state-space model). The methodology is demonstrated using a generic transport model that is excited by one-minus-cosine gust profiles. Comparison with gust responses computed by ZAERO[18] linear panel code serves for verification of the proposed methods, and also to indicate similarities and differences between gust responses computed by a linear and a nonlinear aerodynamic method.

2. Methodology

The aeroelastic equation of motion for an aircraft in response to atmospheric gust excitation, in generalized coordinates, neglecting damping, is stated as:

$$[GM] \{\ddot{\xi}\} + [GK] \{\xi\} - \{GF_A(t)\} = \{GF_G(t)\} \quad (1)$$

where $\{\xi\}$ is the vector of generalized displacements (including rigid body and elastic displacements), and $[GM]$ and $[GK]$ are the generalized mass and stiffness matrices of the structure. $\{GF_A(t)\}$ and $\{GF_G(t)\}$ are the vectors of generalized aerodynamic forces (GAF) and gust generalized aerodynamic forces (GGAF), respectively. The GAF are dependent on the structural deformations, their time histories, and on the time histories of the generalized aerodynamic forces themselves. The GGAF are due to discrete traveling gust excitation. They are dependent on the velocity profile of the gust input, and on the histories of the gust forces. It is important to note that the gust forces are independent of the structural deformations. This implies that the GGAF on the right-hand side of Eq. 1 can be computed separately, before the simulation of Eq. 1, and presented as fixed, time-dependent input vector when simulating Eq. 1. This is unlike the GAFs that must be re-evaluated in every step of the simulation of Eq. 1. When considering CFD tools for gust aeroelastic analysis, this may present significant computational savings, if CFD analysis is only used to compute the GGAF. Of course, in transonic flight, in which the aerodynamic forces are nonlinear functions of flight parameters and elastic structural deformations, CFD may be required also for the computation of the GAF, and it is likely that the GAF and GGAF cannot be computed separately. In such case a fully coupled nonlinear aeroelastic simulation is required. Such simulation is also presented in this manuscript.

In flight conditions in which the elastic response is expected to be linear, CFD analysis can be used only for the computation of the GGAF, on the right-hand side of Eq. 1, while the elastic analysis can be carried out using traditional linear aeroelastic feedback. In flight conditions in which the aeroelastic response is expected to be nonlinear (that is, the aerodynamic forces due to elastic deformations depend nonlinearly on the deformations), Eq. 1 can be integrated fully in a CFD simulation, accounting for all non-linearities. An in between option, for mildly non-linear aeroelastic responses, could be to use CFD-based ROMs for the aeroelastic response of the left-hand side of Eq. 1, as presented in Ref.[11].

The current study presents two methods for CFD-based gust analysis: In the first method, a CFD-based Convolution ROM for the GGAF is computed and used in the aeroelastic simulation of Eq. 1, in which the GAFs are based on traditional, linear, state-space formulation. The second method is that of a full simulation of the aeroelastic equation (Eq. 1) in an elastic CFD analysis. Generalized forces and displacements computed by the two methods are compared. These responses are also compared to a linear gust response simulation performed by the commercial aeroelastic software ZAERO[18].

2.1 Gust Convolution Reduced-Order Model

We consider a discrete gust, with an arbitrary velocity distribution profile f in the flow direction, and a uniform velocity distribution in the spanwise direction. The latter can be expanded straightforwardly to account for non-uniform velocity distribution, for cases of wings of high span. The gust travels over the aircraft at the constant flight speed V , starting from the aircrafts nose at time zero. This gust induces at time t , at location x on the aircraft (x is measured in the flow direction, with origin at the aircrafts nose), a vertical velocity of:

$$w_G(t) = \begin{cases} \bar{w}_G f(t - x/V) & t > x/V \\ 0 & t < x/V \end{cases} \quad (2)$$

where \bar{w}_G is the gust velocity amplitude. A sharp edge gust input profile is defined as a traveling gust of constant vertical velocity, as:

$$w_{SEG}(t) = \begin{cases} \bar{w}_{SEG} & t > x/V \\ 0 & t < x/V \end{cases} \quad (3)$$

$\{GF_{SEG}(t)\}$, the GGAF due to a sharp-edge gust excitation, are simulated in a CFD run. The gust velocities are introduced to the CFD computation, at each time-iteration, by prescribing the gust vertical velocity to all grid points with flow-direction coordinate x of $x \leq tV$. These gust vertical velocities are assigned to the CFD grid time metrics, without actually moving the grid, following the *Field Velocity* method.[9, 13, 14, 17] The generalized forces due to sharp-edge gust are computed at each time step of the CFD analysis according to:

$$\{GF_{SEG}(t)\} = [\phi]^T \{\Psi(t)\} \quad (4)$$

where $\{\Psi(t)\}$ is the aerodynamic transfer function. $\{\Psi(t)\}$ contains the time-dependent aerodynamic forces, computed at the CFD surface grid points, in response to a sharp-edge gust excitation of \bar{w}_{SEG} amplitude. $[\phi]$ is the modal matrix, in which each column represents an elastic mode shape. The mode shapes, which are typically computed by structural finite elements at the finite-element model nodes, are mapped to the CFD surface grids, at which the gust forces are computed, in order to perform the matrix multiplication of Eq. 4. The method used for mode mapping is based on the Infinite Plate Spline method [6], and is implemented in the CFD code [10]. It is noted that the modes of Eq. 4 may be rigid-body or elastic modes, or any other mode shapes. For example, when $\{\phi\}$ is a unit-displacement heave mode, the generalized gust force of Eq. 4 is the time-dependent total lift due to the sharp edge gust. Similarly, the root-bending moment due to the sharp-edge gust can be computed by using a mode that holds the moment arms from each CFD grid to the wing root (a "load mode").

Using the CFD-simulated sharp-edge GGAF, the time history of forces due to arbitrary gust input (the right-hand side of Eq. 1), can be computed via convolution, as:

$$\{GF_G(t)\} = \int_0^t \dot{w}_G(\tau) GF_{SEG}(t-\tau) d\tau \quad (5)$$

where $\dot{w}_G(t)$ is the time derivative of the gust input velocity. The use of convolution according to Eq. 5 assumes that the superposition of gust loads is valid, i.e. the gusts are not too large.

In the current study, gust inputs considered are one-minus-cosine gusts, required by the FAA for aircraft certification. A one-minus-cosine gust input is defined as:

$$w_G(t) = \begin{cases} \frac{1}{2}\bar{w}_G \left(1 - \cos \frac{2\pi(t-x/V)}{L_G/V}\right) & tV - L_G < x < tV \\ 0 & otherwise \end{cases} \quad (6)$$

where L_G is the gust length (in length units).

The GGAF computed by Eq. 5 can be introduced to the right-hand side of the aeroelastic equation of motion (Eq. 1), to form the aeroelastic gust response equation:

$$[GM] \{\ddot{\xi}\} + [GK] \{\xi\} - \{GF_A(t)\} = \int_0^t \dot{w}_G(\tau) GF_{SEG}(t-\tau) d\tau \quad (7)$$

Equation 7 can be solved for ξ using numerical integration schemes. Since the gust excitation force on the right-hand side is independent of the displacements ξ , it can be computed in advance. Also, it is independent of the model used for the estimation of the aerodynamic forces due to elastic deformations on the left-hand side. In the following section the well-known state-space formulation of the aeroelastic equation, with the Minimum-State aerodynamic approximation[3] is used. For completeness the formulation is repeated below.

2..2 State-Space Formulation of the Aeroelastic System

The aeroelastic equation of motion in response to gust excitation (Eq. 1) can be written in state-space form as:

$$\begin{aligned}\dot{x}_S(t) &= \bar{A}_S x_S(t) + \bar{B}_S GF_A(t) + \bar{B}_{SG} GF_G(t) \\ \xi(t) &= \bar{C}_S x_S(t) + \bar{D}_S GF_A(t) + \bar{D}_{SG} GF_G(t)\end{aligned}\quad (8)$$

where x_S is the states vector:

$$x_S(t) = \begin{Bmatrix} \xi \\ \dot{\xi} \end{Bmatrix} \quad (9)$$

and the coefficient matrices are defined as follows:

$$\begin{aligned}\bar{A}_S &= \begin{bmatrix} 0 & 1 \\ -GM^{-1}GK & 0 \end{bmatrix} & \bar{B}_S &= \begin{bmatrix} 0 \\ GM^{-1} \end{bmatrix} & \bar{B}_{SG} &= \begin{bmatrix} 0 \\ GM^{-1} \end{bmatrix} \\ \bar{C}_S &= [I \quad 0] & \bar{D}_S &= [0] & \bar{D}_{SG} &= [0]\end{aligned}\quad (10)$$

The aerodynamic forces due to elastic deformations ($GF_A(t)$) can be written in the Laplace domain as:

$$\{GF_A(s)\} = -q[Q(s)]\{\xi(s)\} \quad (11)$$

where $[Q(s)]$ is the aerodynamic force coefficient (AFC) matrix, and q is the dynamic pressure. AFC matrices are typically available as a function of the reduced frequency $[Q(ik)]$, where k is the reduced frequency, defined as $k = \omega b/V$, where ω is the physical frequency in radians per second, b is the semi-chord length, and V is the flow speed. These are used via rational function approximation to generate a state-space aerodynamic model in the form:

$$[Q(p)] = [A_0] + [A_1]p + [A_2]p^2 + [D]([I]p - [R])^{-1}[E]p \quad (12)$$

where p is the non-dimensional complex Laplace variable $p = \frac{sb}{V}$. Substitution yields:

$$[Q(s)] = [A_0] + \frac{b}{V}[A_1]s + \frac{b^2}{V^2}[A_2]s^2 + [D]\left([I]s - \frac{V}{b}[R]\right)^{-1}[E]s \quad (13)$$

With the formulation of the AFC of Eq. 12, the aeroelastic equation of motion can be written as:

$$\begin{aligned}\dot{x}_{AE}(t) &= \bar{A}_{AE} x_{AE}(t) + \bar{B}_{AEG} GF_G(t) \\ \xi(t) &= \bar{C}_{AE} x_{AE}(t)\end{aligned}\quad (14)$$

where the new state vector is:

$$\{x_{AE}(t)\} = \begin{Bmatrix} \xi \\ \dot{\xi} \\ x_A \end{Bmatrix} \quad (15)$$

and where $\{x_A\}$ is the augmented aerodynamic state vector:

$$\{x_A(s)\} = \left([I]s - \frac{V}{b}[R]\right)^{-1}[E]\{\xi(s)\} \quad (16)$$

and

$$\begin{aligned}\bar{A}_{AE} &= \begin{bmatrix} 0 & I & 0 \\ -\bar{M}^{-1}[GK + qA_0] & -\bar{M}^{-1}\frac{qb}{V}A_1 & -q\bar{M}^{-1}D \\ 0 & E & \frac{V}{b}R \end{bmatrix} \\ \bar{B}_{AEG} &= \begin{bmatrix} 0 \\ \bar{M}^{-1} \\ 0 \end{bmatrix} & \bar{C}_{AE} &= [I \quad 0 \quad 0] & \bar{M} &= GM + \frac{qb^2}{V^2}A_2\end{aligned}\quad (17)$$

Since the gust excitation forces from CFD analysis are provided in discrete time, the state-space aeroelastic equation of motion is also formulated in discrete time, as:

$$\begin{aligned} x_{AE}(n+1) &= A_{AE} x_{AE}(n) + B_{SG} GF_G(n) \\ \xi(n) &= C_{AE} x_{AE}(n) \end{aligned} \quad (18)$$

where

$$A_{AE} = e^{\bar{A}_{AE}T} \quad B_{SG} = \int_0^T e^{\bar{A}_{AE}\tau} d\tau \bar{B}_{SG} \quad C_{AE} = \bar{C}_{AE} \quad (19)$$

Finally, introducing the convolution-based gust excitation force into Eq. 18. The discrete-time state-space aeroelastic system equation of motion in response to gust excitation is written as:

$$\begin{aligned} x_{AE}(n+1) &= A_{AE} x_{AE} + B_{SG} \sum_{k=1}^{n+1} \dot{w}_G(k) GF_{SEG}(n+1-k) \\ \xi(n) &= C_{AE} x_{AE}(n) \end{aligned} \quad (20)$$

3. Numerical Application

3.1 Aircraft Model

The numerical test case is that of a generic transport aircraft. The model includes a fuselage, wing, aileron, and an all-movable tail. The wing and tail are both tapered, and swept aft, with no twist, incidence or dihedral angle. The cross section profiles of the wing and elevator are NACA0012 symmetric airfoils. Table 1 summarizes the wing and tail geometrical dimensions. The fuselage is 20m long with the nose 7.3m forward of the wing leading edge, and the aft end 2.9m behind the tail trailing edge. It has a circular cross section with radius of 0.8m which tapers near the ends. The reference chord is 2m and the reference area is 18m².

Figure 1 presents the structural finite-element model of the aircraft. The wing and tail are modeled by their torsion boxes, which include skin, ribs, spars, and stringers. The fuselage is modeled as a flexible bar. MSC Nastran Modal analysis provided the thirteen low-frequency vibration modes, including two rigid-body modes that were used for gust analysis. ZAERO linear panel model served for validation purposes, for comparison of CFD results with linear-aero results at the linear Mach and angle of attack range. The ZAERO software was also used to generate a state-space aeroelastic model of the aircraft, which served in gust response analysis. The linear panel aerodynamic model includes the wing (flat panel with 14 spanwise strips and 7 chordwise strips), the all-movable tail (flat panel with 6 spanwise strips and 4 chordwise strips), and the fuselage (body element with 42 axial stations and 5 circumferential points on each station). Further details on the linear panel aerodynamic method can be found in Ref. [18].

CFD analysis was performed by the EZNSS code[7]. EZNSS is a finite-difference code, capable of solving the steady or time-accurate Navier-Stokes or Euler equations, using various algorithms. The current study involves mostly time-accurate Euler simulations, using the Steger-Warming solver algorithm. The aeroelastic scheme (elastic deformations, and grid update algorithm following elastic deformations) is presented in Ref.[10].

The airplane was modeled using five overlapping (Chimera) structured grids zones. The grid zones are for the fuselage, wing, and tail surface grids and two Cartesian collar zones that are used for boundary conditions transfer between the wing and fuselage, and tail and fuselage. The total number of grid points is about 570,000. All of the CFD simulations were computed with a non-dimensional time step of 0.01, which corresponds to a real time step of 3.04E-5 seconds.

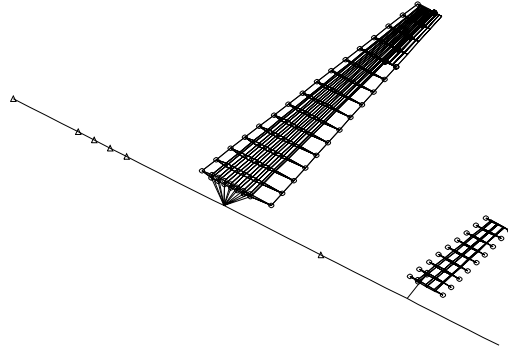


Figure 1: a) Finite element model of the generic transport aircraft

	Wing	Tail
Span [m]	10.0	4.0
Aspect ratio	10.0	6.4
Root chord [m]	3.0	1.5
Leading edge sweep angle [deg]	20.0	20.0
Taper ratio	0.333	0.667

Table 1: Wing and tail geometrical properties

3..2 Forces due to Sharp-Edge and One-Minus-Cosine Gust Excitations

Figure 2 presents the time history of the lift and moment coefficients that develop in response to a sharp-edge gust excitation of equivalent angle of attack of 1 degree, at Mach 0.6, on the rigid aircraft configuration. The time scale is replaced with a normalized time scale $s = tV/b$, where b is the semi-chord length. Since the semi-chord length is taken to be 1, the coefficients history is presented as a function of the gust front location. Figure 2 shows that the aerodynamic forces due to the sharp-edge gust start to develop approximately when the gust front reaches the wing root leading edge. A slight increase in the aerodynamic force values is observed when the gust front reaches the tail. For comparison, figure 2(a) also presents the closed-form Kussner function for the development of the aerodynamic forces on a flat plate in incompressible flow,[1] multiplied by the steady state lift coefficient value. The CFD-computed lift and the closed-form Kussner function are in close agreement, considering the fact that the former is computed for a 3D wing, and the later is computed for a flat plate. The oscillations in lift value, shown in the zoom-in box, are due to convergence of the CFD scheme while the gust travels between one grid-point to the next, in the flow direction. It will be shown that these fluctuations do not affect the computation of responses to arbitrary gust inputs via convolution.

Figure 3 presents the time histories of GGAF associated with the first three elastic modes that develop in response to the sharp edge gust input excitation. Mode 2 is an elevator (tail) mode, hence the relatively small modal forces, and the jump in the response when the gust front hits the elevator. It is noted that in this simulation the aircraft is clamped. That is, only the elastic modes participate in the elastic response. The time histories were simulated over 10,000 CFD iterations (corresponding to 0.305 seconds real time), after which the GGAF are well converged to their final values. The GGAF of figure 3 were used in convolution, according to Eq. 5, to compute the GGAF due to one-minus-cosine gust excitations, as defined by Eq. 6, with gradient lengths of $L_G = 2m$, and $L_G = 50m$, and equivalent amplitude of 1 degree. Figure 4 presents the GGAFs

Figure 2: Aerodynamic coefficients time history in response to a sharp-edge gust of amplitude of 1 degree; Mach 0.6, rigid aircraft configuration

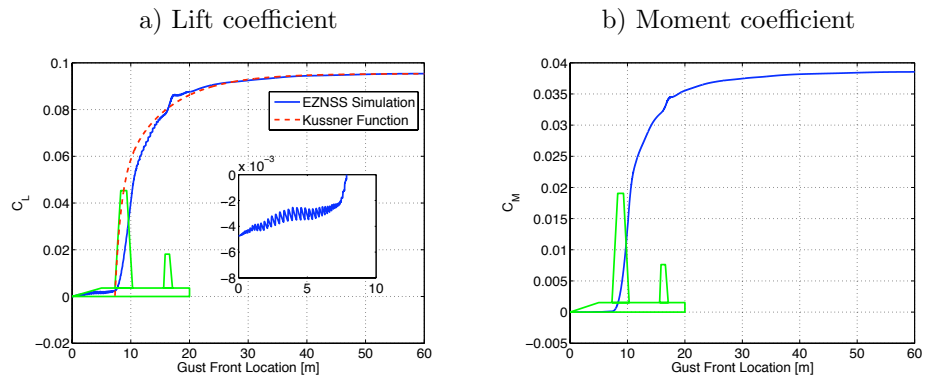
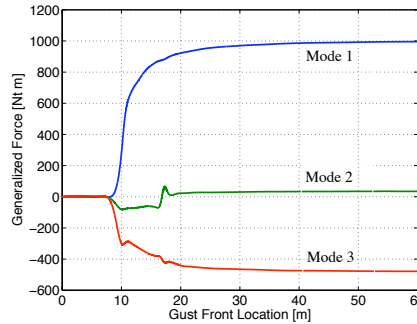


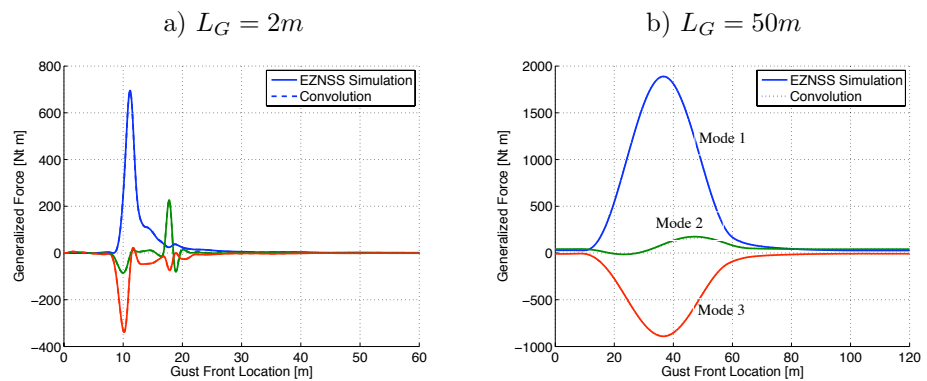
Figure 3: Gust generalized aerodynamic forces in response to a sharp-edge gust of amplitude of 1 degree; Mach 0.6, rigid aircraft configuration



that develop in response to these gust inputs as computed via convolution, compared to the GGAFs computed directly in a CFD simulation. It is evident from figure 4 that for these inputs and flow parameters the convolution captures the response to the gust inputs very accurately. The difference between the convolved and simulated responses is hardly seen in the plots resolution. The convolution therefore offers significant time saving, as only one relatively short CFD simulation is required (that of the sharp-edge response), based on which GGAF due to various excitations can be computed, via convolution, in seconds.

Figure 5 presents comparison of the GGAF computed by EZNSS with those computed by the ZAERO linear panel code, for the same gust inputs of figure 4. The ZAERO code does not output the time history of the GGAF. Instead they were computed from Eq. 1, using the outputted modal elastic deformations from a ZAERO analysis in which the generalized stiffness was set to four order-of-magnitude larger than the real stiffness. By doing so, the inertia term in Eq. 1 becomes negligible, and the GGAF can be computed by multiplying the displacements by the stiffness matrix. Figure 5 shows that the gust forces computed by the ZAERO code are larger than those computed by EZNSS, by about 30% in the two cases presented. This is in correlation with the lift-line

Figure 4: Gust generalized aerodynamic forces in response to a one-minus-cosine gust of amplitude of 1 degree and gradient length of a) 2 m, and b) 50 m; Mach 0.6, rigid aircraft configuration; Computed in EZNSS simulation and via convolution;



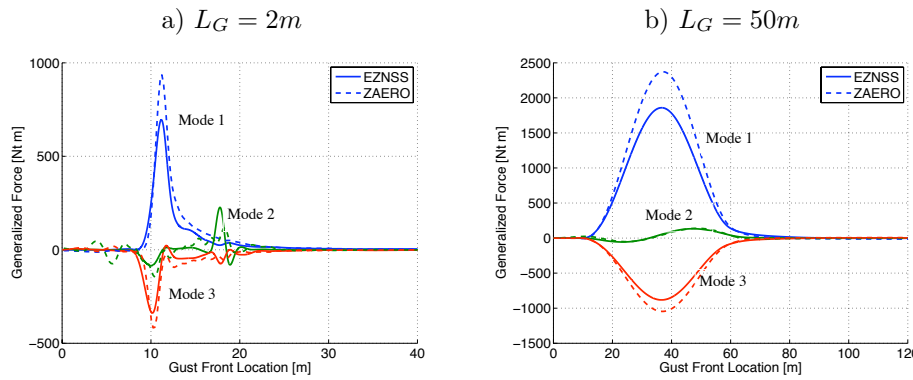


Figure 5: Gust generalized aerodynamic forces in response to a one-minus-cosine gust of amplitude of 1 degree and gradient length of a) 2 m, and b) 50 m; Mach 0.6, rigid aircraft configuration; Computed in EZNSS simulation and with the ZAERO code;

slope of the complete aircraft, which is computed as 0.1 in EZNSS and as 0.12 in ZAERO. This difference in the lift line slope between the two models is rather large for the Mach number considered. It is speculated that this difference stems from modeling issues. It is possible that refinement of any of the CFD or panel grids would yield closer steady lift values. However, the question of accurate lift line slope estimate is not in the scope of this study, as the linear-panel versus CFD gust response comparison is aimed towards comparing the *dynamic* gust response. The time development of the GGAF computed by the two codes is about the same for the slower gust input (figure 5(b)), but for the faster excitation the ZAERO computed GGAF show more dynamic response. These results did not change when the ZAERO GGAFs were computed by increasing the stiffness by five orders-of-magnitude, instead of four.

A state-space discrete-time model of the aeroelastic system was created, using the thirteen structural modal displacements and their time derivatives as states, plus nine augmented aerodynamic lag states, totaling thirty five states. The state-space aeroelastic model was created in ZAERO, based on linear panel method, and was used to compute the gust response according to Eq. 20, with gust excitation forces from CFD analysis. Figure 6 presents responses of the *free elastic aircraft* to one-minus-cosine excitation of gradient length of 2m, equivalent angle of attack of 1 degree, at Mach 0.6, at altitude of 10,000ft (3048m) standard atmosphere. Figure 6(a) presents the response computed by full CFD simulation. Figure 6(b) presents the response from the hybrid method, computed by applying the gust *rigid* forces from CFD (computed via convolution) onto a linear state-space aeroelastic model (from ZAERO), according to Eq. 20. Figure 6(c) presents the response from ZAERO, in which both the aeroelastic model and the gust forces are based on linear aerodynamics. Figure 6(d) presents a comparison of first mode only response as computed via full CFD simulation and ZAERO linear analysis. It shows that the *initial* development of gust response, including the time when the response is at its peak, is computed similarly with the CFD and linear methods. The magnitude of the max modal displacement computed by ZAERO is larger than that computed by EZNSS. This is consistent with the differences in the static aerodynamic coefficients computed by the two codes. For longer simulation times the responses deviate, due to the different development of rigid body motions. It is noted that the rigid body motion of this aircraft is uncontrolled, and therefore diverges, and is not expected to be similar in the two computations. It doesn't affect the estimation of the maximum loads, which occurs at shorter simulation times, for which the rigid body motions are still small.

The elastic response from the hybrid analysis and from ZAERO analysis are similar in nature, because they both originate from the same aeroelastic model. However the magnitude of response in the hybrid analysis reflects the CFD-based rigid input and is thus smaller than the ZAERO linear response. Considering the fact that the aircraft structural analyst or designer are likely

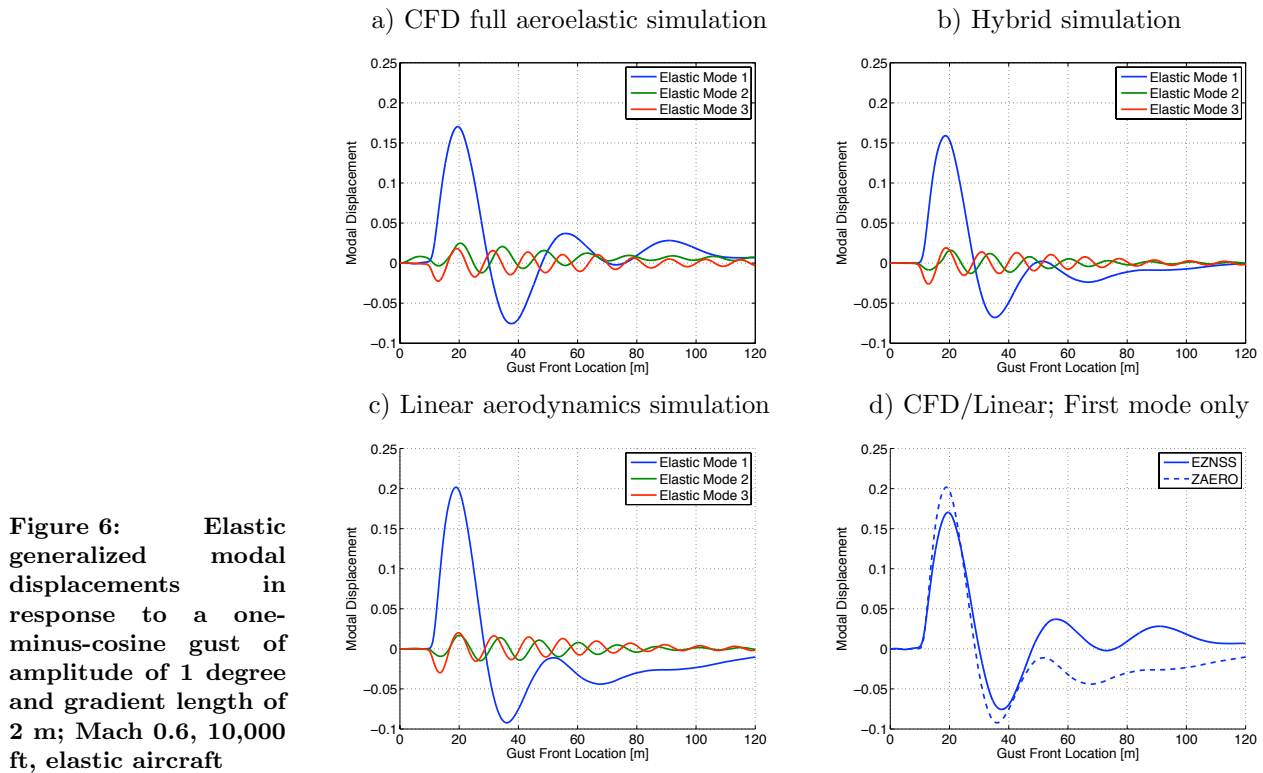


Figure 6: Elastic generalized modal displacements in response to a one-minus-cosine gust of amplitude of 1 degree and gradient length of 2 m; Mach 0.6, 10,000 ft, elastic aircraft

to be interested in the magnitude of the max response, and its time, the hybrid method, which is based on a state-space linear elastic model fed by CFD-based rigid gust forces, offers an accurate and very computationally efficient analysis option. Figure 7 presents similar responses for a one minus cosine gust of 50m length.

4. Summary

The study presents two approaches for computing gust response of elastic free aircraft configuration based on CFD analyses. The *direct* approach involves full aeroelastic simulation within the CFD run. The *hybrid* approach involves computing rigid sharp-edge gust responses in a CFD run, computing the gust input forces due to arbitrary gust profiles via convolution, and applying a linear aeroelastic feedback loop to compute the aeroelastic gust responses. The latter is highly computationally efficient, as only one relatively short CFD run is required for the computation of the sharp-edge gust responses, after which responses to arbitrary gust profiles can be computed in seconds. The former is more elaborate and time consuming, and can be used in nonlinear flight conditions, such as flight in the high transonic regime, or at very low speeds close to stall, where the flow is detached. Comparisons with gust responses computed by a linear panel code validated the proposed methods, and highlighted the differences in gust responses computed by the panel and CFD codes. While the aeroelastic responses computed by the two codes were found to be relatively similar in frequencies and damping, the modal displacements predicted by the linear panel code were larger than those predicted by the CFD code. This suggests that in this case a structural design for gust loads the use of panel and CFD codes may yield different designs. Future studies will further explore the *hybrid* method for various flight regimes. For flight conditions in which the flow may be nonlinear, but the elastic deformations may be small and therefore the elastic response may be linearized, it is possible that the *hybrid* method may be still applied with CFD-based ROMs replacing the currently used linear GAFs. This is currently

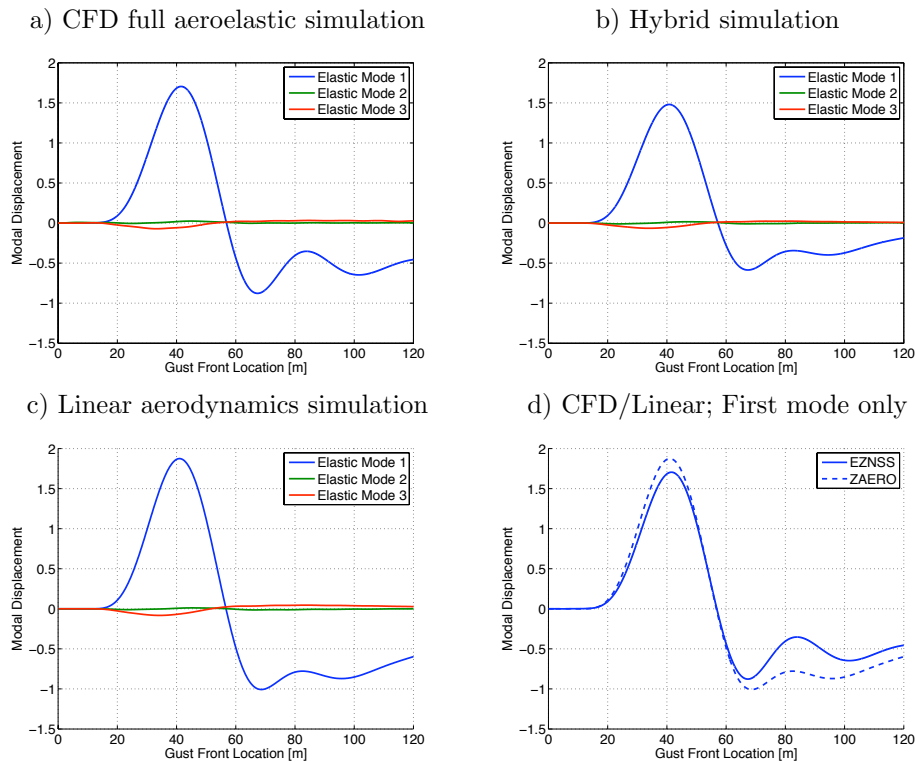


Figure 7: Elastic generalized modal displacements in response to a one-minus-cosine gust of amplitude of 1 degree and gradient length of 50 m; Mach 0.6, 10,000 ft, elastic aircraft

being studied by the author, together with a study of the applicability of the linear convolution concept in transonic flight conditions.

References

- [1] R. L. Bisplinghoff, H. Ashley, and R. L. Halfman. "Aeroelasticity". Dover Publications, Inc., Mineola, NY, 1996.
- [2] M. Gennaretti and F. Mastroddi. "Study of Reduced-Order Models for Gust-Response Analysis of Flexible Wings". *Journal of Aircraft*, 41(2), 2005.
- [3] M. Karpel. "Design for Active Flutter Suppression and Gust Alleviation Using State-Space Aeroelastic Modeling". *Journal of Aircraft*, 19(3):221–227, 1982.
- [4] M. Karpel, B. Moulin, L. Anguita, C. Maderuelo, and H. Climent. "Aeroservoelastic Gust Response Analysis for the Design of Transport Aircrafts". In *45th Structures, Structural Dynamics and Materials Conference*, Palm Springs, CA, 2004. AIAA.
- [5] M. Karpel, B. Moulin, and P. C. Chen. "Dynamic Response of Aeroservoelastic Systems to Gust Excitation". *Journal of Aircraft*, 42(5):1264–1272, 2005.
- [6] Harder R. L. and Desmarais R. N. Interpolation Using Surface Splines. *Journal of Aircraft*, 9(2):189–191, 1972.
- [7] Y. Levy. "Numerical Simulation of Dynamically Deforming Aircraft Configurations using Overset Grids". *Journal of Aircraft*, 38(2):349–354, 2001.
- [8] T. E. Noll, J. M. Brown, M. E. Perez-Davis, D. I. Stephen, G. C. Tiffany, and M. Gaier. "Investigation of the Helios Aircraft Mishap". Technical report, NASA, 2004.

- [9] V. Parameswaran and J. D. Baeder. "Indicial Aerodynamics in Compressible Flow - Direct Computational Fluid Dynamics Calculations". *Journal of Aircraft*, 34(1):131–133, 1997.
- [10] D. Raveh, Y. Levy, and M. Karpel. "Structural Optimization Using Computational Aerodynamics". *AIAA Journal*, 38(10), 2000.
- [11] D. E. Raveh. "Identification of Computational-Fluid-Dynamics Based Unsteady Aerodynamic Models for Aeroelastic Analysis". *Journal of Aircraft*, 41(3):620–632, 2004.
- [12] D. E. Raveh. "CFD-Based Models of Aerodynamic Gust Response". *Journal of Aircraft*, 44(3):888–897, 2007.
- [13] R. Singh and J. D. Baeder. "Direct Calculation of Three-Dimensional Indicial Lift Response Using Computational Fluid Dynamics". *Journal of Aircraft*, 34(4):465–471, 1997.
- [14] R. Singh and J. D. Baeder. "Generalized Moving Gust Response Using CFD with Application to Airfoil-Vortex Interaction". In *15th AIAA Applied Aerodynamics Conference*, Atlanta, GA, 1997. AIAA.
- [15] D. Tang, D. Kholodar, J. Jer-Nan, and E. H. Dowell. "System Identification and Proper Orthogonal Decomposition Method Applied to Unsteady Aerodynamics". *AIAA Journal*, 39(8):1569–1576, 2001.
- [16] G. Yang and S. Obayashi. "Numerical Analyses of Discrete Gust Response for an Aircraft". *Journal of Aircraft*, 41(6):1353–1359, 2004.
- [17] A. Zaide and D. Raveh. "Numerical Simulation and Reduced-Order Modeling of Airfoil Gust Response". *AIAA Journal*, 44(8):1826–1834, 2006.
- [18] Zona Technologies, Inc., Scottsdale, AZ. *ZAERO Theoretical Manual*, Nov. 2003.